CONF-791077--4

THE DISTRIBUTION OF ^{241}Am IN THE HUMAN BODY AS DETERMINED BY EXTERNAL COUNTING

by

R. E. Toohey

Prepared for

Workshop on

Measurement and Interpretation of Actinide Accumulation by Man

Snowbird, Utah

October 14-18, 1979

U of C-AUA-USDOE

ARGONNE NATIONAL LABORATORY, ARGONNE, ILLINOIS

Operated under Contract W-31-109-Eng-38 for the U. S. DEPARTMENT OF ENERGY

DISCLAIMER

The facilities of Argonne National Laboratory are owned by the United States Government. Under the terms of a contract (W-31-109-Eng-38) among the U. S. Department of Energy, Argonne Universities Association and The University of Chicago, the University employs the staff and operates the Laboratory in accordance with policies and programs formulated, approved and reviewed by the Association.

MEMBERS OF ARGONNE UNIVERSITIES ASSOCIATION

The University of Arizona
Carnegie-Mellon University
Case Western Reserve University
The University of Chicago
University of Cincinnati
Illinois Institute of Technology
University of Illinois
Indiana University
Iowa State University
The University of Iowa
Kansas State University
The University of Kansas
Loyola University
Marquette University
Michigan State University
The University of Michigan
University of Minnesota
University of Missouri
Northwestern University
University of Notre Dame
The Ohio State University
Ohio University
The Pennsylvania State University
Purdue University
Saint Louis University
Southern Illinois University
The University of Texas at Austin
Washington University
Wayne State University
The University of Wisconsin

79-20-1

THE DISTRIBUTION OF ^{241}Am IN THE HUMAN BODY AS DETERMINED BY EXTERNAL COUNTING*

R. E. Toohey
Center for Human Radiobiology
Argonne National Laboratory
Argonne, IL 60439

Abstract

Methods for determining the distribution of ^{241}Am within the body of a contaminated subject and their application to several cases under study at the Center for Human Radiobiology are described. In general, ^{241}Am is found in the lungs even at long times after inhalation, and systemic ^{241}Am is observed to deposit in the liver and to label the skeleton in a fairly uniform manner; similar findings have been reported in animal studies (L172). Further analysis of the skeletal distribution of ^{241}Am indicates deposition on bone surfaces. In contrast, the distribution of injected ^{239}Pu in an (abnormal) skeleton is rather non-uniform when compared to that of ^{241}Am.

---

* Work supported by U.S. Department of Energy.

Introduction

^{241}Am is an α-emitting radionuclide with a half-life of 458 y. A 60-keV γ-ray accompanies 36% of the α-decays, and neptunium L x-rays centered at about 18 keV also occur following internal conversion. Animal data have indicated the uptake of ^{241}Am by the liver and skeleton (Ll72, Th70, Co73), and the few reported instances of human exposure (To79, Wr72, Fr76, Pa79) have indicated the same. The maximum permissible body burden is 50 nCi, with bone as the critical organ (ICRP60). The maximum permissible lung burden is 15 nCi, calculated by the methods of ICRP.

Because of the paucity of human data, as much information as possible must be obtained from each case, both for the benefit of the individual concerned and to contribute to our knowledge of the metabolism of this radionuclide by the human body. A major part of this desired information concerns the distribution of activity within the body. Fortunately there are methods available

for determining the distribution in all three spatial directions. These methods include scanning techniques for distribution measurements along the length and width of the body, and a variety of methods to determine the actual or effective depth of the activity in the body as viewed by an external detector. Unfortunately, the severe attenuation by bone and soft tissue of the photons emitted by ^{241}Am contributes greatly to the difficulty of both collecting and interpreting the distribution information.

This paper will discuss the various techniques for determination of the distribution, and will report the distributions of ^{241}Am in several individuals examined at the Center for Human Radiobiology. Finally the distributions of ^{241}Am and ^{239}Pu in the human skeleton will be compared.

Measurement Techniques

The simplest method of obtaining distribution

information is by scanning - simply recording the counting rate observed with a detector in different positions along the body. These measurements may be done with large, unshielded detectors at widely separated locations, as in the "seven-position scan" technique of Miller (Mi64), or with a well-collimated detector placed successively at adjacent, narrowly-separated locations to obtain a "profile scan."

Fig. 1 shows seven-positions scans taken with detectors above and below the supine body of case 30-041, a worker who contained approximately 0.9 μCi of ^{241}Am, originally inhaled as $^{241}AmO_2$ (To76a). Even though the results of these scans provide relatively little detail they contain a surprising amount of distribution information. For example, the higher counting rates from the upper crystal at positions 5 and 6 indicate activity in the bones of the legs, and especially in the knees, since more soft tissue shields the lower crystal

than the upper, even though the legs are much closer to the lower crystal than to the upper.

These scans also indicate that much of the activity in the thorax is actually in the lungs for the following reasons: 1) a higher counting rate is observed from the back than from the front; 2) the maximum counting rate appears to be nearer the vertex when measured from the front than from the back; and 3) a broader peak in the counting rates is observed from the back than from the front. All these characteristics can be predicted from a consideration of the size, shape and positioning of the lungs in the thoracic cavity.

In the profile scan technique either a 20-mm wide collimator, or a focused-slit collimator, is placed over the detector, yielding a spatial resolution of about 100 mm at the mid-plane of the body. This resolution is demonstrated in Fig. 2, a longitudinal profile scan of case 30-063, a subject who contained two point sources of ^{241}Am of the

type used in domestic smoke detectors (Ru77). Each source contained about 2.5 μCi of ^{241}Am, and they were observed to be in the gastro-intestinal tract, lying at about 560 mm and 680 mm from the vertex, respectively. The two sources were easily resolved by the scanning technique.

The other type of distribution information, namely the effective depth of the activity in the body, is obtained by analysis of the photon spectrum collected by an external detector over any location on the body. All of the methods take advantage of the phenomenon of Compton scattering. As the amount of low-Z scattering material lying between a given amount of ^{241}Am and the detector is increased, fewer 60-keV photons reach the detector without losing some of their energy in one or more collisions with electrons in the scattering material. This increase in the ratio of scattered to primary photons detected offers a means of determining the thickness of

scattering material traversed.

If the photon detector has sufficient resolution, the scattered photons are well separated from the primary peak. For example, in the case of a xenon-filled proportional counter, the ratios of counts in the energy bands 35-45 keV (To75) or 35-55 keV (Ya73) to those in the 60-keV peak have been found to be linearly dependent on the thickness of tissue-equivalent absorber overlying the source, up to about 120 mm.

In the case of NaI(Tℓ) detectors, the scattered photons are not resolved from the primaries, so different methods are used. The 60-keV peak may be divided into two parts, and the ratio of counts in the lower energy part to those in the higher energy part has also been found to depend linearly on the thickness of tissue-equivalent absorber overlying the source (To76b). Alternatively, the shift of the observed centroid of the peak to a lower energy or the increase in peak width may

be used as the parameter to indicate overlying absorber thickness (Wr72). The depth determination techniques with an NaI(Tℓ) crystal are not as sensitive as that with a xenon-filled proportional counter, as shown in Fig. 3.

Finally, it must be noted that because the sources normally present in vivo are distributed rather than point, the above techniques usually determine an effective, rather than actual, depth for the source. This effective depth is then used to derive the approximate calibration factor for the detection system either by measurements of point sources and absorber (To76a), or by adjusting a phantom to conform to the subject (Wr72).

Applications and Discussion

The techniques described above have been applied to data previously obtained on two cases of ^{241}Am inhalation: 30-001, an adult male, and 30-002, a ten-year-old boy; these cases have been described in detail elsewhere (Ru72, Wr72). The data are summarized in Fig. 4. The

upper graph shows intensity measurements made with the 7-position scan technique in which position 4 is at the midpoint of the body. The lower graph shows the effective depth of ^{241}Am in the two subjects at each position. The importance of the depth determinations for calibration is demonstrated by the measurements on 30-001 in positions 4 through 7. The intensity measurements are quite constant for these four positions, while the depth measurements show a variation of almost a factor of three. The effective depths measured are consistent with what would be expected from anatomical considerations.

Further information about the distribution of activity in the thorax of case 30-041 (Fig. 1) can be obtained from transverse profile scans, shown in Fig. 5 (To79). The uppermost diagram in Fig. 5 is a scan made with the slit of the collimated detector parallel to the spine and centered at 0.4 m from the vertex. In order to remove the contribution of ^{241}Am in the spinal column from this scan, another scan

was made 0.2 m further down the body. At this point the detector was away from the major portion of the lung tissue, but still under part of the rib cage. This second scan is shown in the middle portion of Fig. 5 and the difference between the two scans is plotted in the lower portion. The two peaks remaining when the contribution from bone is removed confirm the presence of activity in the lungs. The asymmetry which results from the fact that the right lung is larger than the left is typically observed in cases of inhaled activity. The contribution from activity in the liver is negligible for this case because of chelation therapy, but in general, activity in the liver would interfere with measurements of this kind.

The distribution of ^{241}Am in the skeleton of this case can be derived from the results of longitudinal profile scans, shown in Fig. 6, along with a scale drawing of the skeleton for reference. The large peak at 0.4 m

from the vertex is due to ^{241}Am in both bone and lung, as shown above, and the peaks at 1.3 and 1.75 m from the vertex suggest deposition on bone surface. (The ends of the long bones are primarily trabecular in nature while the shafts are primarily cortical bone.) In order to analyze the skeletal distribution, the data were divided into five regions as shown in Fig. 6.

The amount of bone surface area in each region was calculated from the values of cortical and trabecular bone mass for 15 groups of bones given for Reference Man (ICRP75). Since cortical bone accounts for 4 kg of bone mass and 5 m^2 of bone surface area, and trabecular bone accounts for 1 kg of mass and 5 m^2 of area, the total surface area for each group equals 1.25 m^2/kg times the cortical mass plus 5 m^2/kg times the trabecular mass. Table 1 shows the percent of bone surface area, % total counting rate and % corrected counting rate (for the 1977 data) in each of the five regions. The corrected

counting rate was obtained by subtracting from region II the contribution due to ^{241}Am in the lungs. [This lung content was determined independently from measurements made over the thorax with a xenon-filled proportional counter, which in turn was calibrated by determining the effective depth of the material in the thorax. The lung content was determined to be between 5 and 10% of the amount originally inhaled, some 12 years after the inhalation (To79).] The correlation coefficient of the corrected counting rates and bone surface areas (columns 3 and 4 of Table 1) is + 0.96. This latter number is significant at the 99.5% level (for three degrees of freedom) and this offers striking confirmation of the deposition of ^{241}Am on bone surfaces.

Some additional information on the distribution of ^{241}Am in the body of this case is available from measurements of activity in the liver. These measurements were made by placing the proportional counter over the

right side of the abdomen at a distance of 0.65 m from the vertex and tilted 45° from the vertical so as to be roughly parallel to the surface of the body. The counting rate obtained was then compared with that observed when the counter was in a similar position over the left side of the abdomen. The counting rate ratio was 1.03 ± 0.02 while the subject was still on chelation therapy, with very little activity in the liver. The ratio increased to 1.09 ± 0.03 one year after the cessation of chelation, and to 1.31 ± 0.04 after another two years. The increase in the ratio indicates that in the absence of chelation therapy, ^{241}Am is being deposited in the liver after its removal from bone or lung. Because of the severe attenuation by tissue of the photons emitted from ^{241}Am in the liver, it is extremely difficult to calibrate the counter. A crude estimate of the activity in the liver is 25 nCi, which is not deemed sufficient to justify the resumption of chelation therapy at this time.

Comparison of the Skeletal Distributions of ^{241}Am and ^{239}Pu

As noted above, the skeletal distribution of ^{241}Am in case 30-041 is quite uniform and well-correlated with the distribution of bone surface area. This does not appear to be true for ^{239}Pu in the skeleton of case 40-010, who received 0.3 μCi of ^{239}Pu by intravenous injection in 1945. At the time of injection, this subject was suffering from Cushing's syndrome with its accompanying osteoporosis, and consequently, her skeleton may be considered abnormal. The distribution of ^{239}Pu in her skeleton has been reported by Larsen et al. (La78). In general, for any one bone, plutonium was more highly concentrated in the trabecular portion than in the cortical portion, but overall, the concentration of plutonium in the axial skeleton was an order of magnitude greater than that in the appendicular skeleton.

The fifth column of Table 1 gives the percent of total skeletal plutonium found in those bones of case 40-010 which lie in each of the five regions defined for case 30-041.

The correlation coefficient of bone surface area and plutonium content (columns 4 and 5) is equal to + 0.87. This number is still significant, but only at the 95% level. The differences in ^{241}Am and ^{239}Pu content are most apparent in regions IV and V, which include portions of only the appendicular skeleton.

The skeletal distribution (both macro- and microscopic) of ^{239}Pu in case 40-010 and another injection case, 40-015, are presented in more detail in contributions to these proceedings by Larsen et al. (La79) and Schlenker et al. (Sc79), and so will not be discussed further here.

It is of interest to note that dissimilarities in the skeletal distributions of ^{241}Am and ^{239}Pu have been observed in beagles (Ll72), in that the ^{241}Am was deposited uniformly on all bone surfaces, but ^{239}Pu was deposited preferentially on endosteal surfaces rather than periosteal, and in general was not as uniformly distributed as ^{241}Am. However, it seems

unlikely that the difference in microscopic distribution can account for the large variations in macroscopic distribution presented in Table 1.

Summary

A significant amount of information regarding the distribution and therefore the metabolism of ^{241}Am can be obtained by external counting in vivo. Among our findings are the retention of 5 to 10% of the originally inhaled amount in the lungs at 12 years after inhalation; the initial deposition of ^{241}Am in the liver, its removal by chelation therapy, and its gradual re-deposition in the liver after cessation of chelation therapy; and a uniform labelling of the skeleton by ^{241}Am, with a highly significant correlation between bone surface and ^{241}Am content for various regions of the skeleton. This uniform skeletal deposition of ^{241}Am contrasts with that of ^{239}Pu, which, although also depositing on bone surfaces, seems to be concentrated in the more metabolically-active portions of the skeleton.

References

Co73 Cohen N. and Wrenn M. E., 1973, "Metabolic Characteristics of ^{241}Am in the Adult Baboon", Radiat. Res. 55, 129.

Fr76 Fry F. A., 1971, "Long-term Retention of Americium-241 Following Accidental Inhalation", Health Phys., 31, 13.

ICRP60 International Commission on Radiological Protection, 1960, "Report of Committee II on Permissible Dose for Internal Radiation", Health Phys., 3, 146.

ICRP75 International Commission on Radiological Protection, 1972, "Reference Man", Publication 23, p. 67 (Oxford: Pergamon Press).

La78 Larsen R. P., Oldham R. D., Cacic C. G., Farnham J. E. and Schneider J. R., 1978, "Distribution of Injected Plutonium in the Skeleton and Certain Soft Tissues", Argonne National Laboratory Radiological and Environmental Research Division Annual Report, July 1977-June 1978, ANL-78-65, Part II, pp. 145-153.

La79 Larsen R. P., Oldham R. D. and Toohey R. E., 1979, "Macro-Distribution of Plutonium in the Human Skeleton", these proceedings.

Ll72 Lloyd R. D., Jee W. S. S., Atherton D. R., Taylor G. N. and Mays C. W., 1972, "Americium-241 in Beagles: Biological Effects and Skeletal Distribution", in: Radiobiology of Plutonium, B. J. Stover and W. S. S. Jee, eds. J. W. Press, Salt Lake City, pp. 141-148.

Mi64 Miller C. E., 1964, "A New Technique for Determining the Distribution of Radium and Thorium in Living Persons", Assessment of Radioactivity in Man, Proc. Symp. Heidelberg, 1964, IAEA Vienna, Vol. 1, pp. 67-77.

Pa79 Palmer H. E. and Rieksts G. A., 1979, "In Vivo Measurement of Americium-241 in the Hanford Americium Accident", presented at the 24th Annual Meeting of the Health Physics Society, Philadelphia, PA, 8-13 July 1979, abstract P/62.

Ru72 Rundo J., Keane A. T. and May H. A., 1972, "Measurement of Americium-241 in a Ten-Year Old Boy", in: Assessment of Radioactive Contamination in Man, Proc. Symp. Stockholm, 1972, Vienna: IAEA, pp. 579-594.

Ru77 Rundo J., Fairman W. D., Essling M. and Huff D. R., 1977, "Ingestion of ^{241}Am Sources Intended for Domestic Smoke Detectors: Report of a Case", Health Phys. 33, 561.

Sc79 Schlenker R. A. and Oltman B. G., 1979, "Plutonium Micro-Distribution in Human Bone", these proceedings.

Th70 Thomas R. J., 1970 "Estimation of ^{241}Am Body Burdens by Analysis of Whole-Body Scanning, Excreta and Body Weight Data", Health Phys. 29, 417.

To75 Toohey R. E., 1975, "An Experimental Method of Estimating the Depth of ^{241}Am Deposited in the Chest", Health Phys. 29, 417.

To76a Toohey R. E. and Essling M. A., 1976, "Gross Distribution of ^{241}Am in Man Seven Years after Inhalation", in: Biological and Environmental Effects of Low-Level Radiation, Proc. Symp. Chicago, 1975, Vienna: IAEA, Vol. II, pp. 153-160.

To76b Toohey R. E. and Rundo J., 1976, "A Rapid Method for Estimating the Effective Depth of Internally-Deposited Americium-241", in: Diagnosis and Treatment of Incorporated Radionuclides, Proc. Symp. Vienna, 1975, Vienna: IAEA, pp. 278-281.

To79 Toohey R. E. and Essling M. A., 1979, "Measurements of ^{241}Am in Vivo at Long Times after Inhalation", Health Phys., in press.

Wr72 Wrenn M. E., Rosen J. C. and Cohen N., 1972, "In-Vivo Measurements of Americium-241 in Man", Proc. Symp. Stockholm, 1972, pp. 595-618 (Vienna: IAEA).

Ya72 Yaniv S. S., Brodsky A. and Sashin D., 1972, "Analysis of Pu-Am Spectra in a Xe Proportional Counter: Effect of Characteristic X-rays", Health Phys. 23, 705.

Table 1.

Comparison by region of the observed fractions of the ^{241}Am counting rate from case 30-041, the available bone surface area, and the ^{239}Pu content of the skeleton of case 40-010. The regions are defined in Fig. 6.

	30-041			40-010
Region	% ^{241}Am total counts	% ^{241}Am less lung	% bone surface	% ^{239}Pu content
I	13	15	12	18
II	37	23	26	34
III	20	25	33	39
IV	16	19	17	5
V	15	18	12	3

Figure captions

Figure 1: Seven-position scans of case 30-041, obtained with two uncollimated 292-mm diameter by 102-mm thick NaI(Tℓ) detectors, one above and one below the supine subject. Position 4 is at the midpoint of the subject's height and the remaining positions are 267 mm apart, along the length of the body. (Fig. 1 of To76a).

Figure 2: Longitudinal profile scan of case 30-063, obtained with a single collimated 292-mm diameter by 102-mm thick NaI(Tℓ) detector below the supine subject. (Fig. 1 of Ru77).

Figure 3: Ratios of scattered-to-primary 60-keV photons as a function of absorber thickness overlying a source of ^{241}Am. (Fig. 1 of To75).

Figure 4: Seven-position scans (upper frame) and derived effective source depths (lower frame) for cases 30-001 and 30-002, taken with a single uncollimated detector below the supine subjects. (Fig. 3 of To76b).

Figure 5: Transverse profile scans of the thorax of case 30-041, obtained with a single collimated 292-mm diameter by 102-mm thick NaI(Tℓ) detector below the supine subject at 400 and 600 mm from the vertex, and their difference. (Fig. 2 of To79).

Figure 6: Longitudinal profile scans of case 30-041, obtained with a single collimated detector below the supine subject. The three scans, taken in 1973, 1975 and 1977, show that there has been no extensive re-distribution of activity during this time period. The counting rates and skeleton have been divided into five regions for analysis of the distribution of activity. (Fig. 1 of To79).

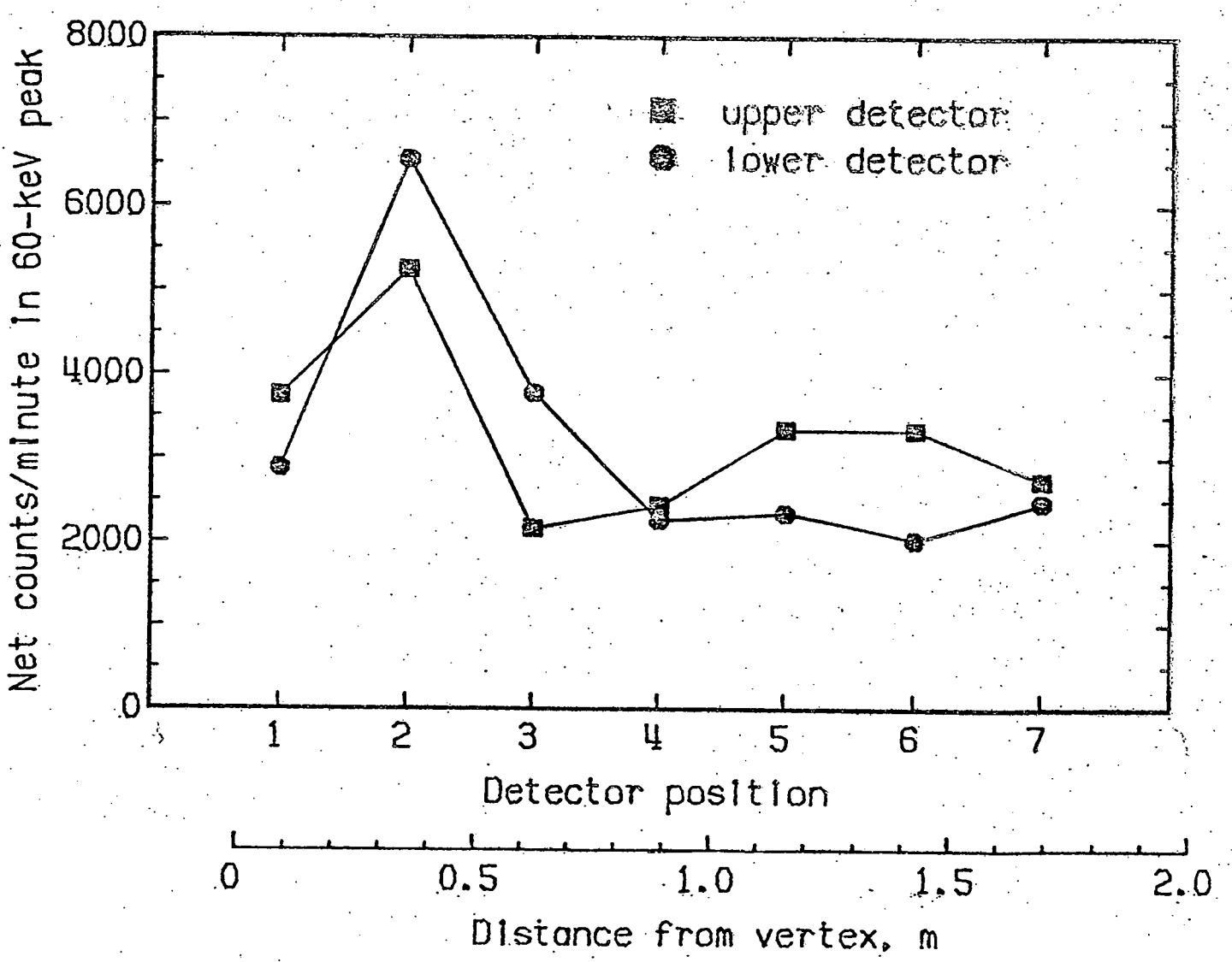
8000
6000
4000
2000
0
Net counts/minute in 60-keV peak
upper detector
lower detector
1
2
3
4
5
6
7
Detector position
0
0.5
1.0
1.5
2.0
Distance from vertex, m

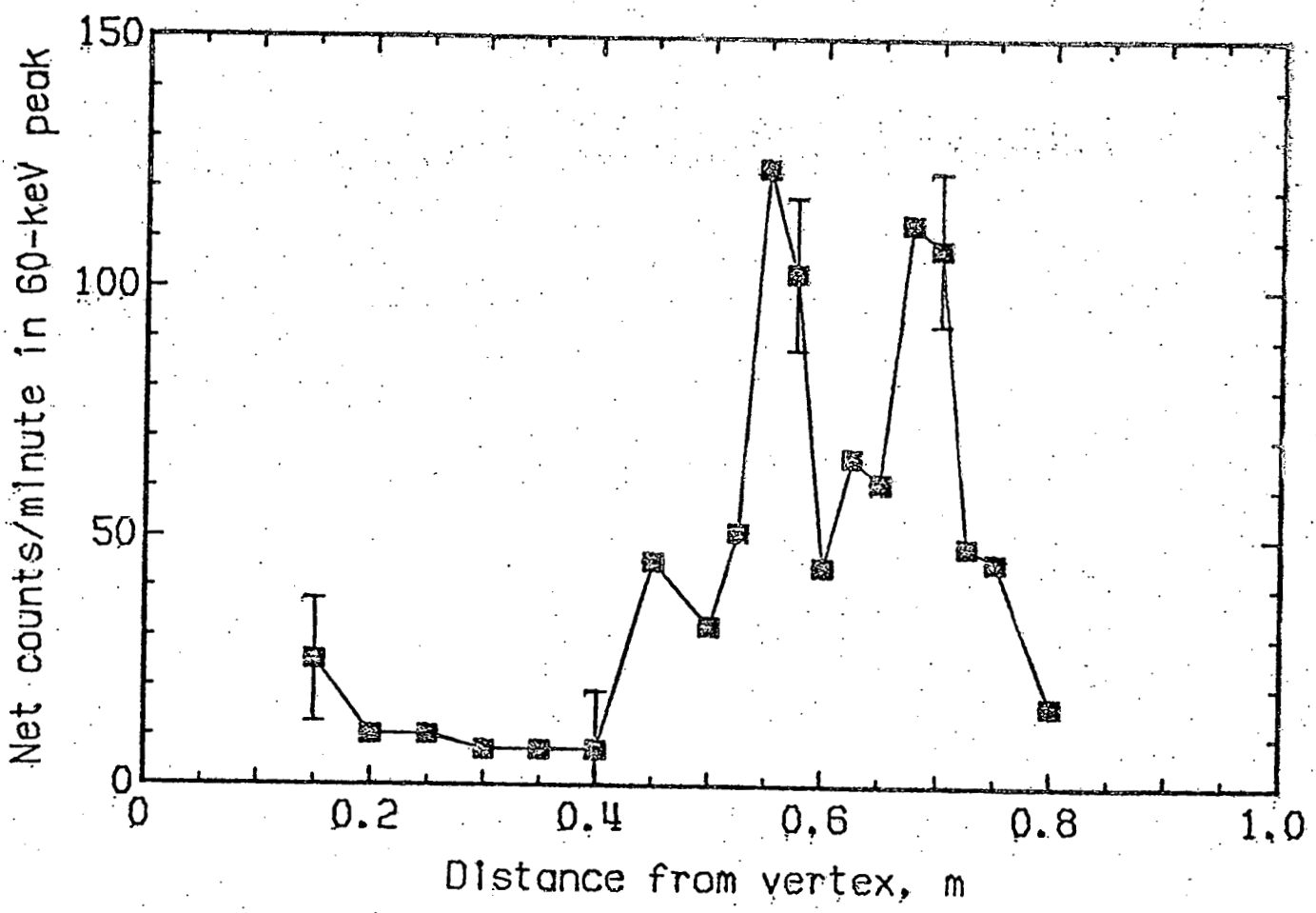
Net counts/minute in 60-keV peak
150
100
50
0
0
0.2
0.4
0.6
0.8
1.0
Distance from vertex, m

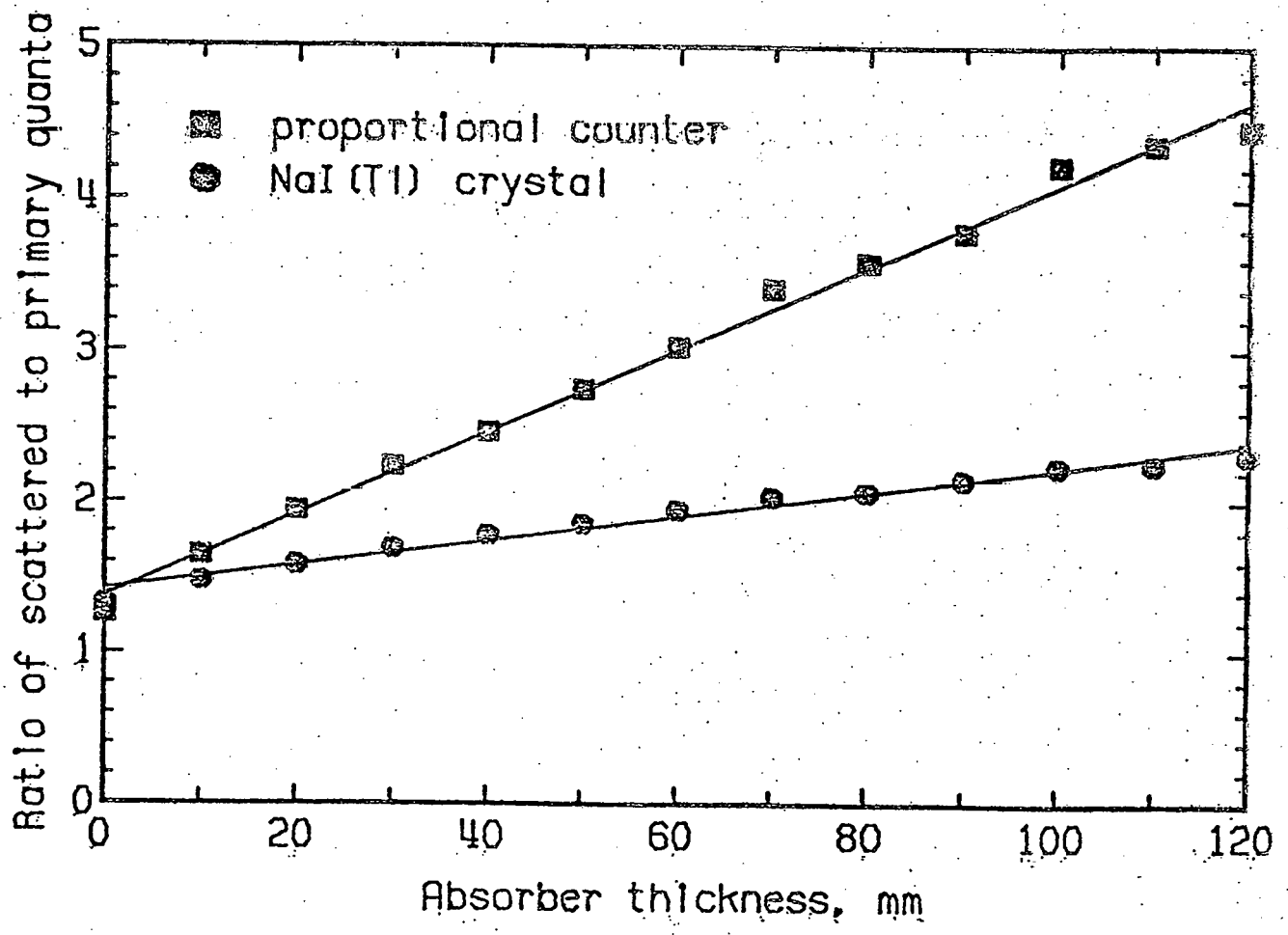
proportional counter
NaI (Tl) crystal
Ratio of scattered to primary quanta
Absorber thickness, mm
0
1
2
3
4
5
0
20
40
60
80
100
120

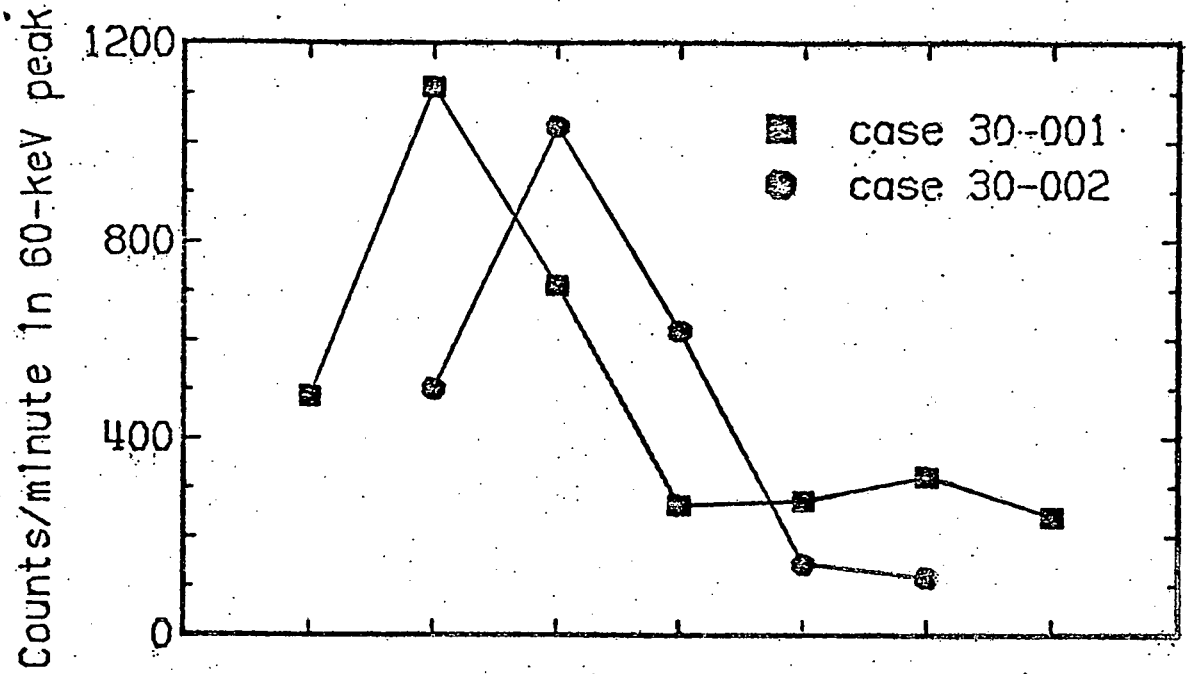
Counts/minute in 60-keV peak
1200
800
400
0
case 30-001
case 30-002

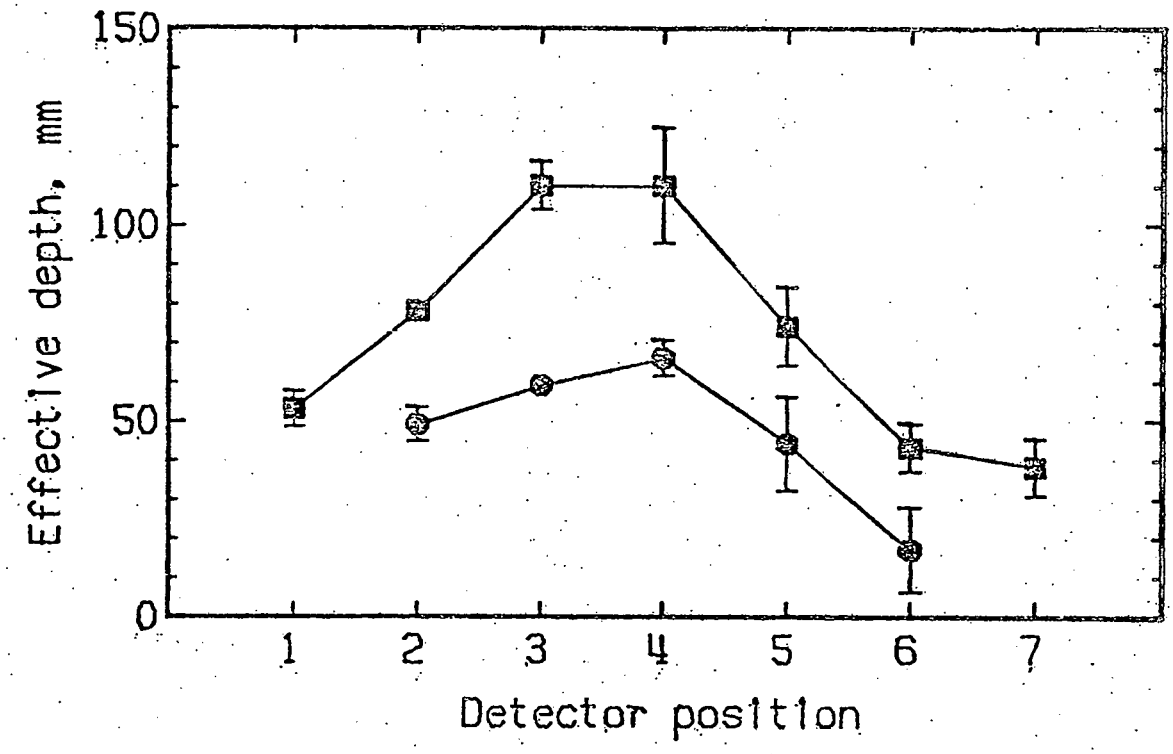
Effective depth, mm
150
100
50
0
1
2
3
4
5
6
7
Detector position

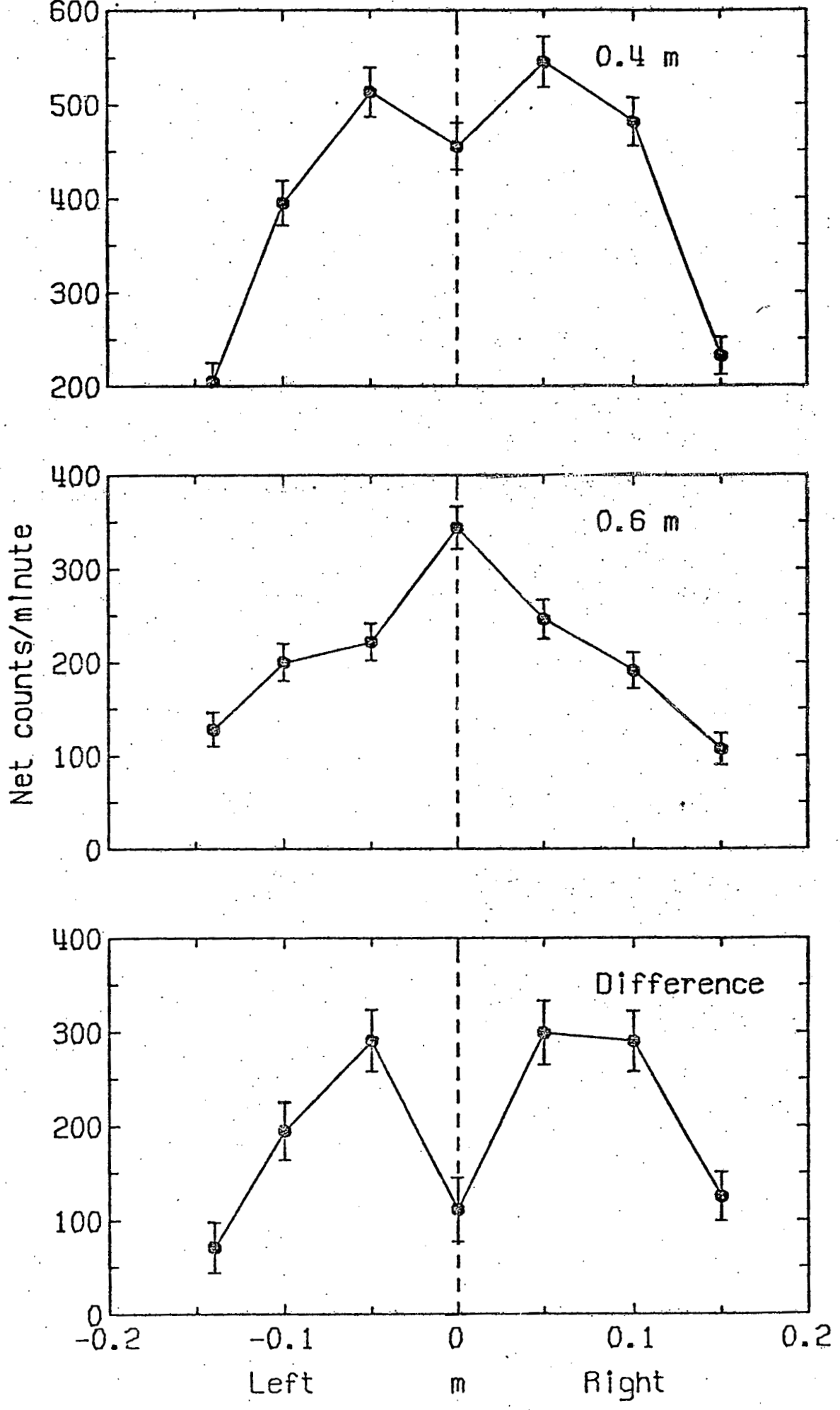
0.4 m
0.6 m
Difference
Net counts/minute
600
500
400
300
200
400
300
200
100
0
400
300
200
100
0
-0.2
-0.1
0
0.1
0.2
Left
m
Right

⑥

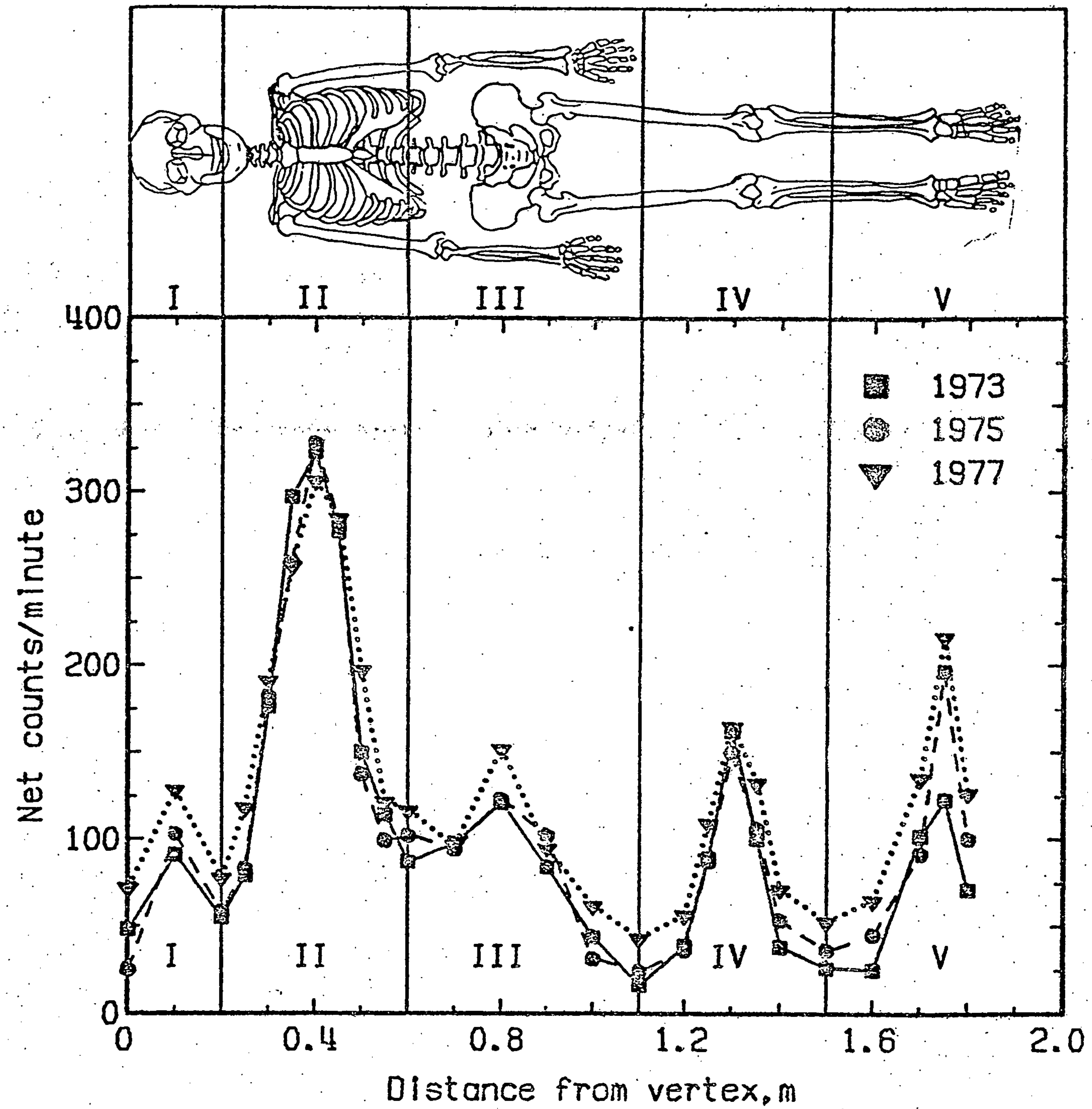

ANL-78-65-II ... Fig 8 48%

149-78-414 7/8735

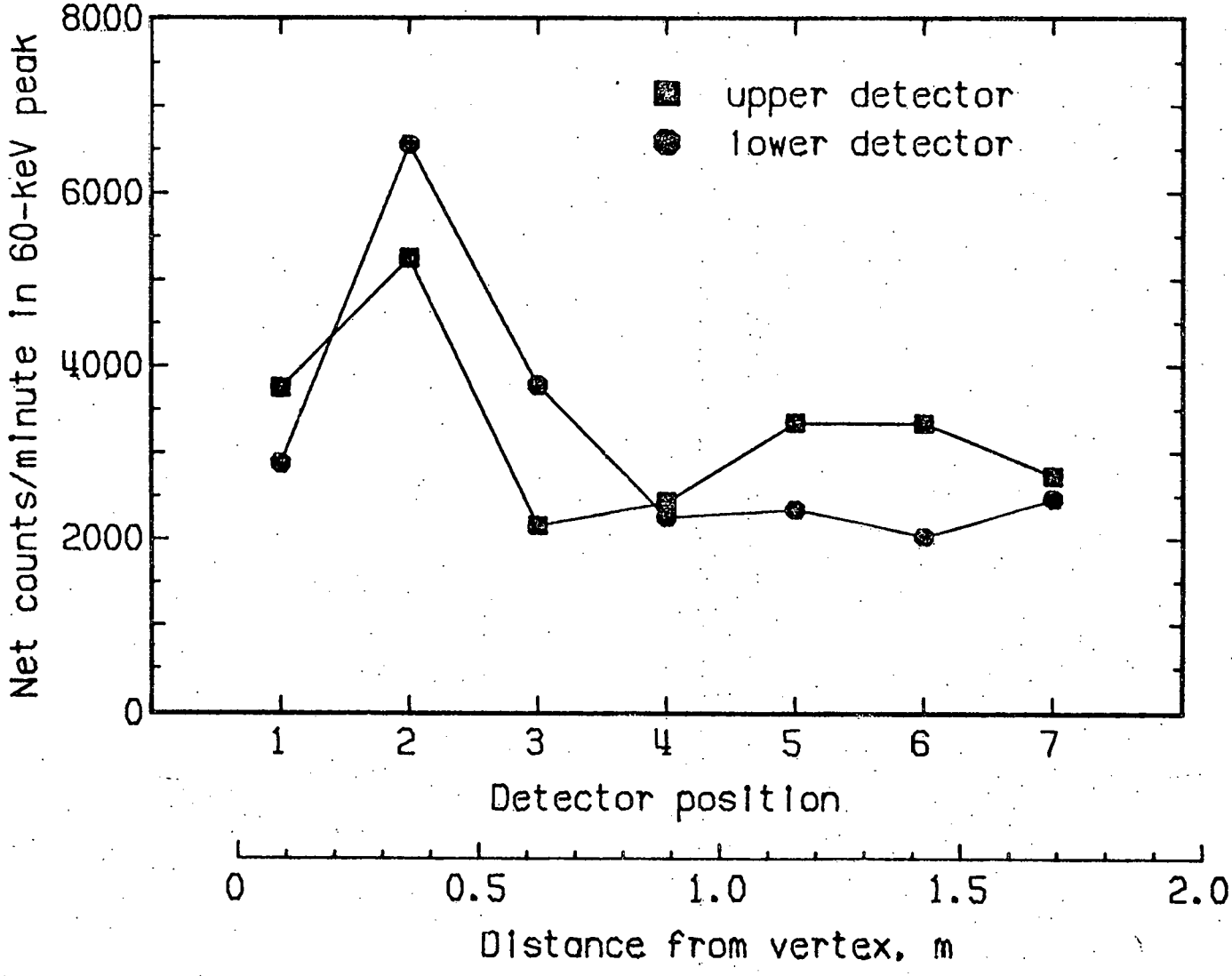
8000
6000
4000
2000
0
Net counts/minute in 60-keV peak
upper detector
lower detector
1
2
3
4
5
6
7
Detector position
0
0.5
1.0
1.5
2.0
Distance from vertex, m

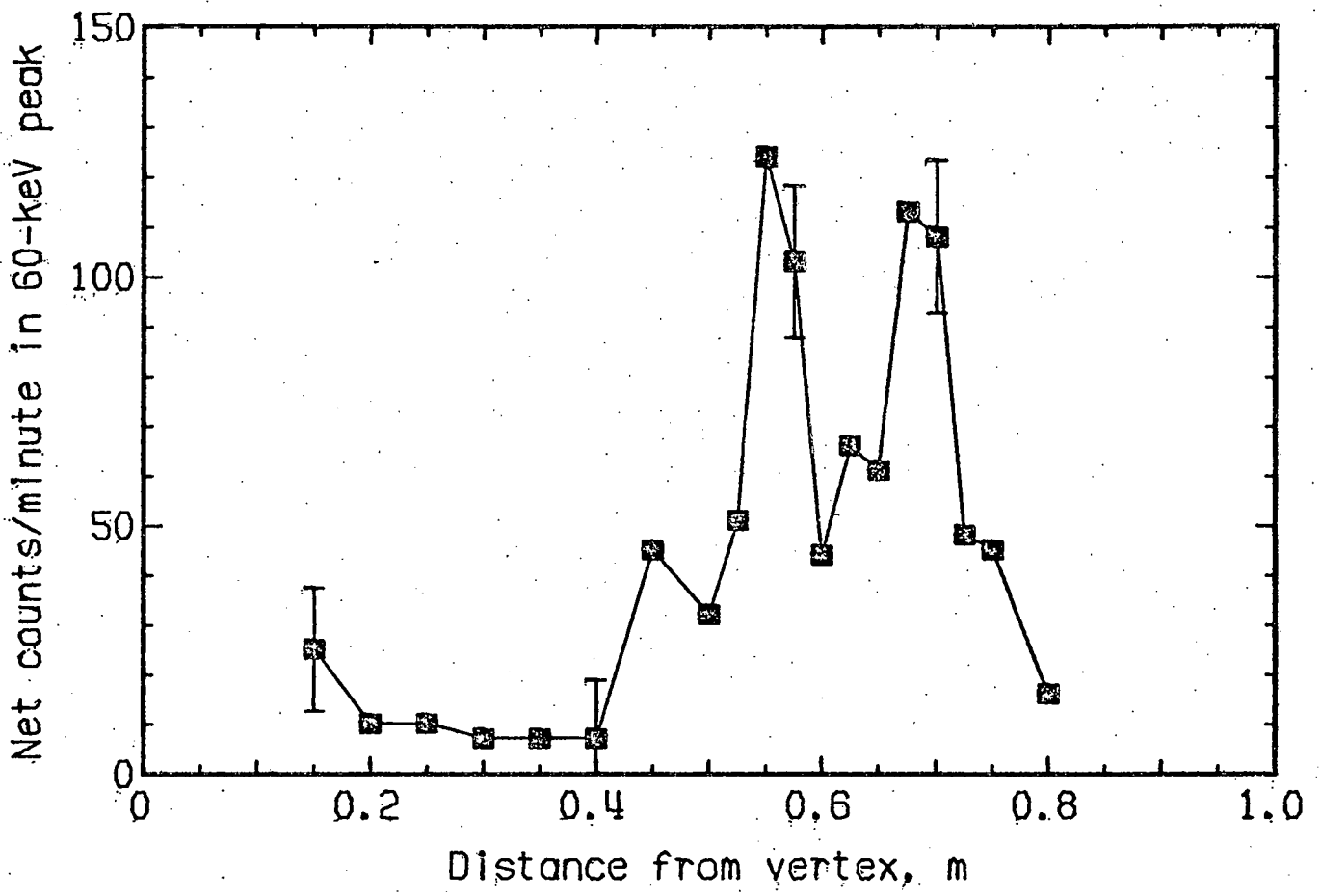
150
100
50
0
0
0.2
0.4
0.6
0.8
1.0
Net counts/minute in 60-keV peak
Distance from vertex, m

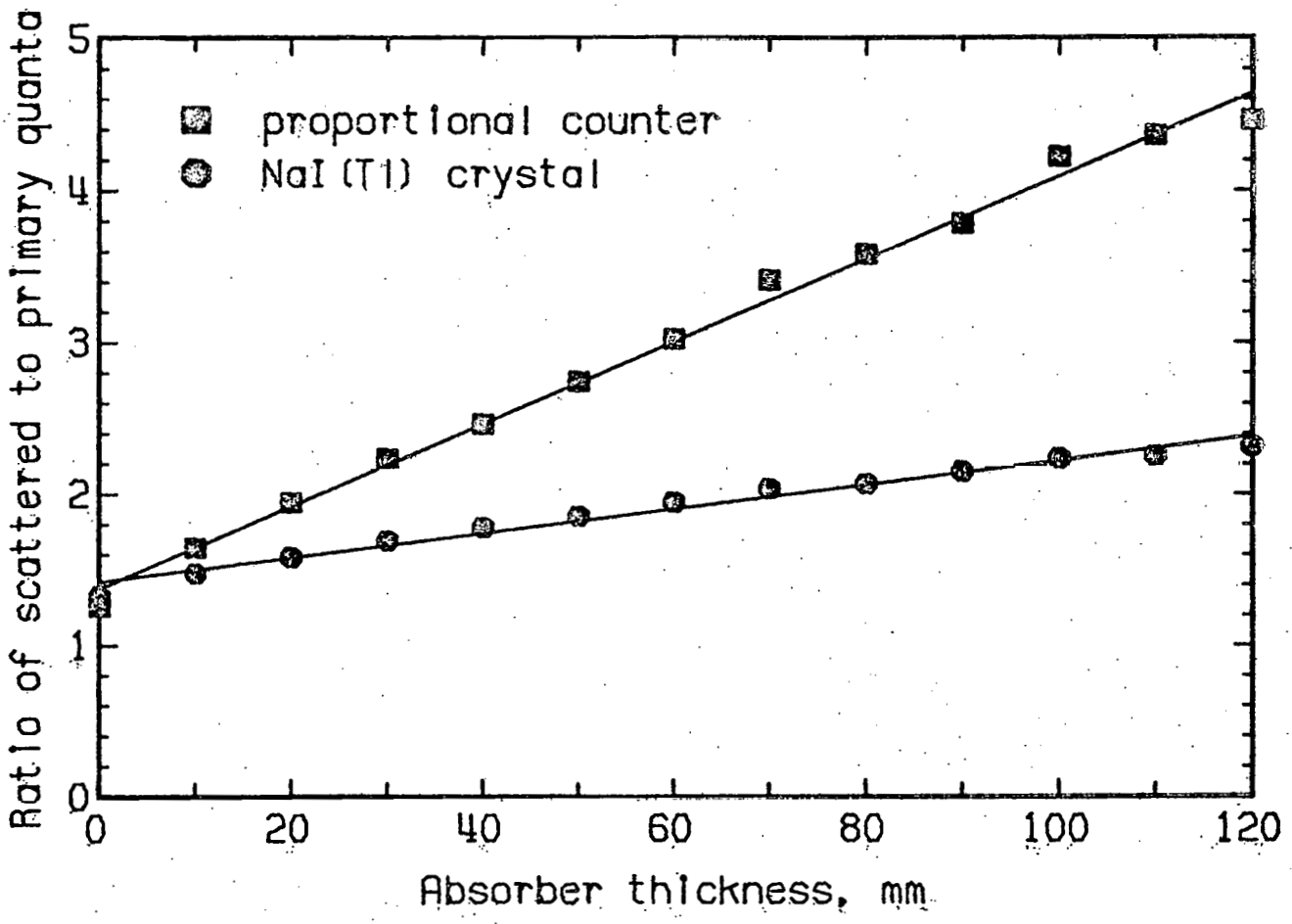
proportional counter
NaI (Tl) crystal
Ratio of scattered to primary quanta
Absorber thickness, mm
0
1
2
3
4
5
0
20
40
60
80
100
120

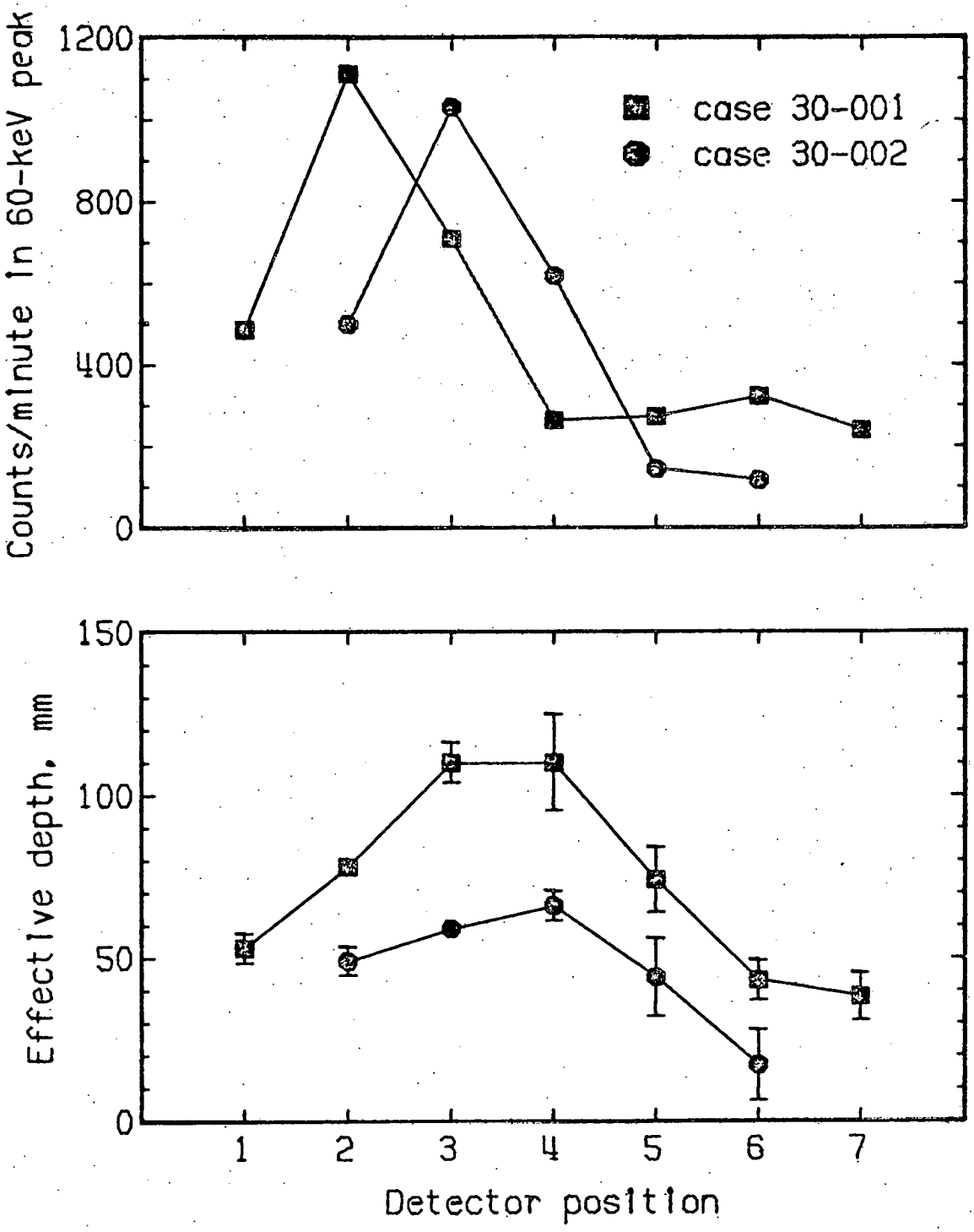
Counts/minute in 60-keV peak
1200
800
400
0
case 30-001
case 30-002
Effective depth, mm
150
100
50
0
1
2
3
4
5
6
7
Detector position

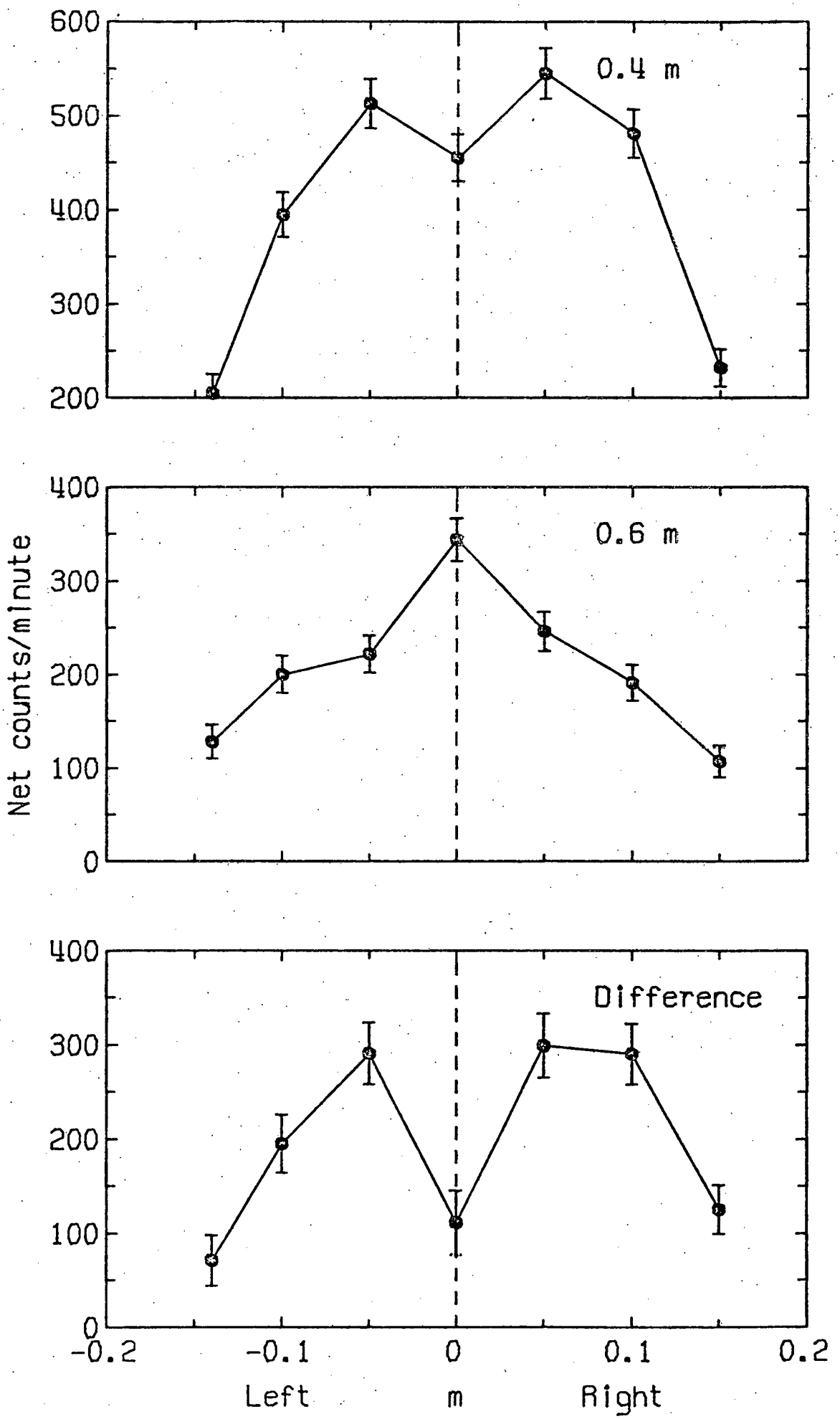
0.4 m
0.6 m
Difference
Net counts/minute
600
500
400
300
200
100
0
-0.2
-0.1
0
0.1
0.2
Left
m
Right

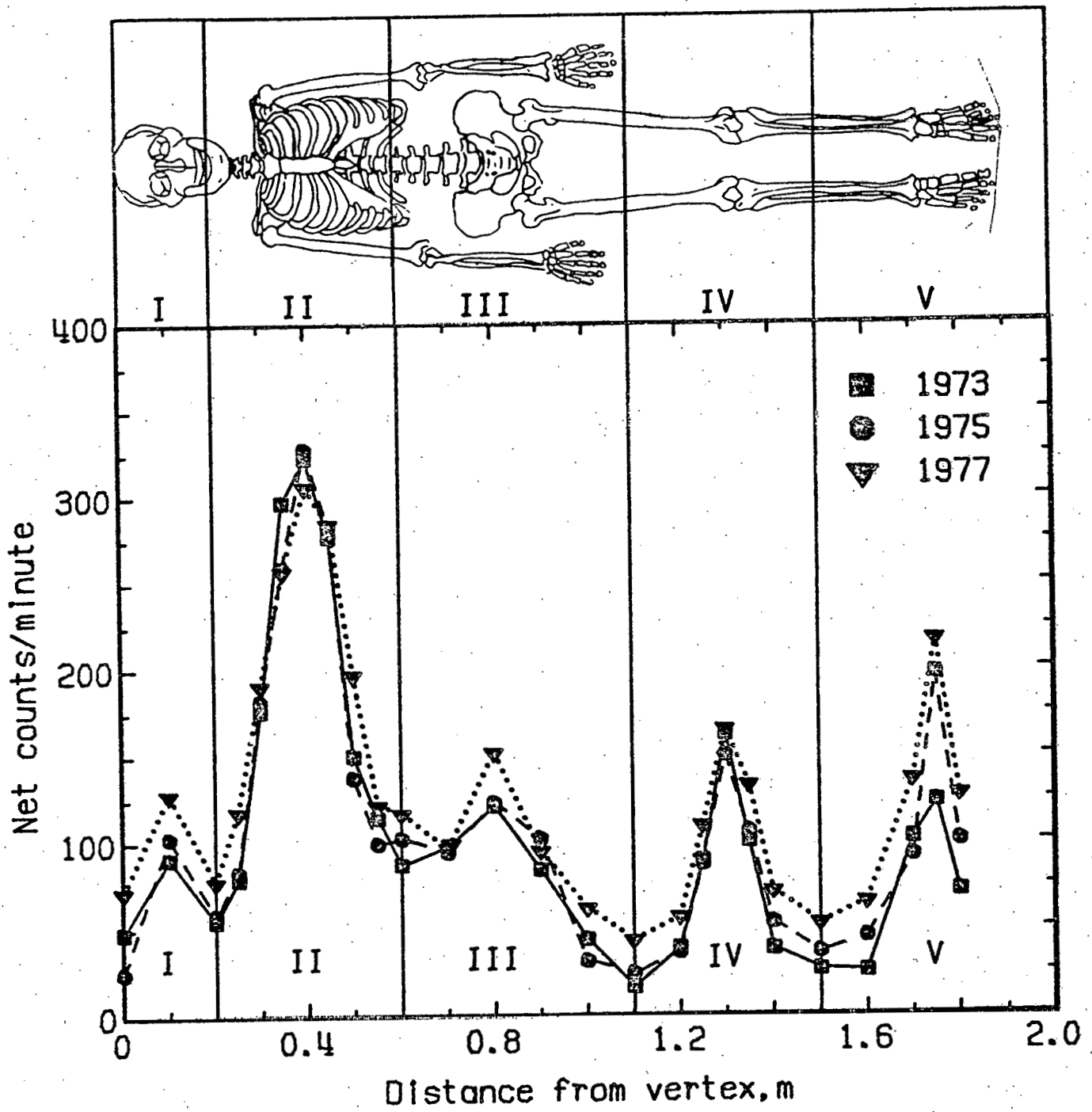

48%

149-78-1414

7/8735